epl A Letters Journal Exploring the Frontiers of Physics

June 2007

EPL, **78** (2007) 68007 www.epljournal.org
doi: 10.1209/0295-5075/78/68007

Drag on a sphere moving through an aging system

H. Tabuteau[1], F. K. Oppong[1], J. R. de Bruyn[1] and P. Coussot[1,2]

[1] *Department of Physics and Astronomy, University of Western Ontario - London, ON N6A 3K7, Canada*
[2] *Institut Navier - Paris, France*

received 4 January 2007; accepted in final form 7 May 2007
published online 4 June 2007

PACS 82.70.-y – Disperse systems; complex fluids
PACS 83.60.La – Viscoplasticity; yield stress
PACS 64.70.Pf – Glass transitions

Abstract – We have investigated the drag on a sphere falling through a clay suspension that has a yield stress and exhibits rheological aging. The drag force increases with both speed and the rest time between the preparation of the system and the start of the experiment, but there exists a non-zero minimum speed below which steady motion is not possible. We find that only a very thin layer of material around the sphere is fluidized when it moves, while the rest of the suspension is deformed elastically. This is in marked contrast to what is found for yield-stress fluids that do not age.

Pasty materials and concentrated suspensions have microscopic internal structure which gives them the ability to resist shear. They can behave as soft solids or shear-thinning fluids, depending on the stress applied [1]. When the force F on an object in the material is less than a critical value F_c, the material responds as a solid and the object will not move. When $F > F_c$, the material around the object becomes fluidized and it moves [2,3]. Pasty materials can easily develop strain heterogeneities such as shear banding [4] and many different pasty materials exhibit similar rheological aging behavior [5]: their rheological properties, and in particular the yield stress, change with time due to slow evolution of the microstructure. The dynamics of this evolution is similar to that of glasses [5,6], and in some cases aging can result in a fluid-solid transition. Aging has been studied in several yield-stress materials [7,8], but most thoroughly in model systems which exhibit strong aging effects and have a relatively simple microstructure [8].

The motion of particles through pasty materials is important in many applications [1], and drag has been studied to some extent in yield-stress systems that do not age [2,3,9,10]. The drag force on a sphere of radius R moving through a yield-stress fluid is given by

$$F = -\int_{S_c} (\mathbf{T}\cdot\hat{e})\cdot\hat{x}\,\mathrm{d}s. \tag{1}$$

$\mathbf{T}$ is the stress tensor and S_c the material surface on which the yielding criterion is met [1]; S_c separates the solid and liquid regions in the material surrounding the sphere. $\hat{e}$ is the outward-pointing unit vector at S_c and $\hat{x}$ a unit vector in the direction of the motion. In simple shear, the stress τ and shear rate $\dot{\gamma}$ *without aging* can be related by the Herschel-Bulkley model, $\tau/\tau_c = 1 + (K/\tau_c)\,\dot{\gamma}^n$, where τ_c is the yield stress and K and n are material parameters. The drag force can be written similarly [10]:

$$F/F_c = 1 + (K/\tau_c)\,\dot{\gamma}_{app}^n \tag{2}$$

for $F > F_c$. F_c, the minimum force required for steady motion in the liquid regime, has been calculated [2] to be

$$F_c = 4\pi R^2 \tau_c k_c \tag{3}$$

with $k_c = 3.5$. The apparent shear rate $\dot{\gamma}_{app} = v/\ell$, where v is the sphere's speed and $\ell = 1.35\,R$ for $n = 0.5$ [10]. With these values for k_c and ℓ, eq. (1) indicates that, in the absence of aging, S_c is approximately R from the sphere's surface. Experiments with a non-aging yield-stress fluid agreed well with these theoretical results [3]. The effect of aging on drag has received little attention, however [11,12]. Ferroir *et al.* have studied the motion of a sphere falling through a thixotropic clay suspension as a function of age and developed a theoretical model for the observed behavior [11]. Recently, Gueslin *et al.* used particle imaging velocimetry to investigate the flow field in a similar system [12]. Nonetheless drag in aging materials remains poorly understood from both the macroscopic and microscopic points of view.

Here we study the drag on a weighted ping-pong ball of diameter $2R = 3.96\,\mathrm{cm}$ falling through a clay suspension

that exhibits rheological aging. Since the sphere falls through previously undisturbed material, its motion at a time t probes the properties of the suspension at that time and provides a direct measure of the changes in properties as the suspension ages. We find that the drag force increases with both v and the waiting time t_w between preparation of the sample and the start of the experiment, and that v approaches a non-zero value as F approaches the critical force F_c. By comparing the drag measurements with rheological data, we show that the sphere moves through the material by fluidizing a very thin layer of the suspension —much smaller than R— immediately surrounding it, while the rest of suspension is deformed elastically. This is very different from the situation in non-aging materials [3].

We worked with Laponite RD [13], a synthetic clay frequently used as a model aging material [8]. It consists of disk-shaped particles 30 nm in diameter and 1 nm thick. We mixed the clay 3% by weight with deionized water, adding NaOH to raise the pH to 10. The resulting suspension, with density $\rho_l = 1012\,\mathrm{kg/m^3}$, was stored in a sealed container for four weeks to ensure complete hydration of the clay particles. Thorough remixing before each experiment was critical for obtaining reproducible results. A combination of local mixing with a hand-held blender and large-scale mixing with a propeller-blade mixer operating continuously at 300 rpm destroyed the suspension's microstructure and put it in a reproducible initial state. After remixing, the material was left to age for a waiting time t_w, during which its microstructure partially reformed, then the experiment was started.

The ping-pong ball had a small hole cut into it, and its density ρ_s was changed by gluing small steel beads inside it. Apart from a small piece of tape at the top to cover the hole, its surface roughness was on the order of 10 μm. This is much larger than the particle size, so slip at the sphere's surface is not expected to be important. It was dropped into the suspension from 1 cm above the free surface and its position recorded at up to 250 frames per second. The experimental container was square in cross-section, with width $L = 20\,\mathrm{cm}$ and depth 45 cm. For our value of $2R/L = 0.2$, the effect of the walls is to increase the effective drag force on the sphere by at most 10% [14,15]. Since the wall effects are small and constant in all of our experiments, neglecting them has no effect on our results.

After an early-time regime dominated by inertia, the sphere either slows to a steady terminal velocity or stops, as shown in the inset to fig. 1(a). We focus on later times, when inertial effects can be neglected. Figure 1(a) shows the sphere's penetration depth D (scaled by R) as a function of time t for different values of ρ_s and a fixed t_w[1].

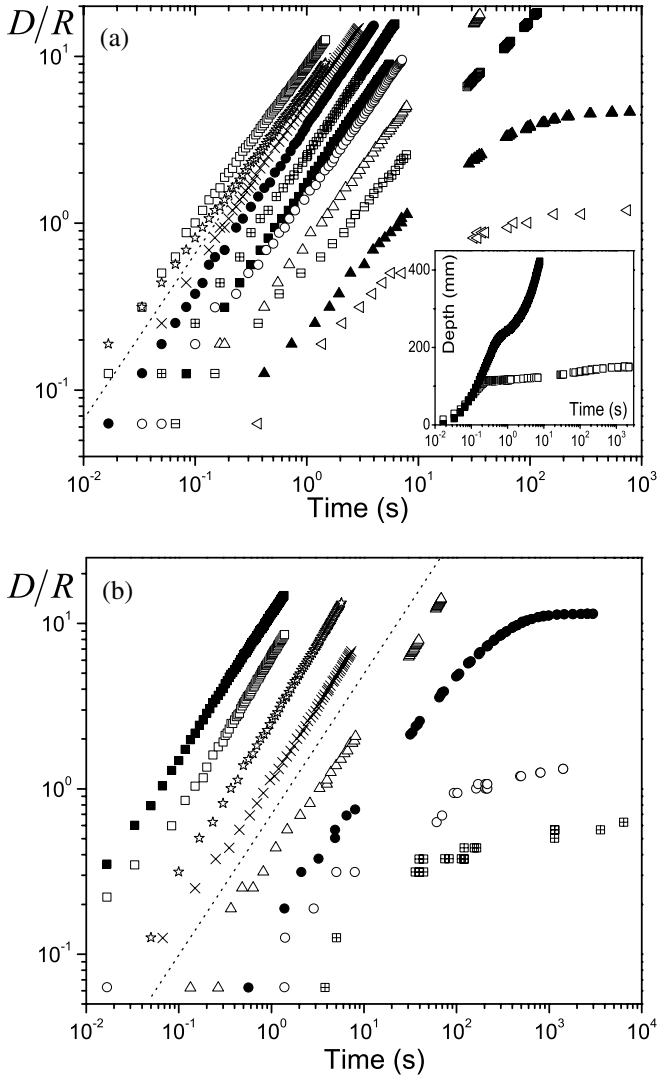

Fig. 1: (a) Scaled penetration depth D/R *vs.* time t for the sphere falling through the Laponite suspension for (left to right) $\Delta\rho = 1589$, 1524, 1460, 1389, 1319, 1251, 1153, 1057, 956, and 890 kg/m^3. Here $t_w = 4$ min. The dotted line has a logarithmic slope of 1, corresponding to a constant speed. The inset shows D as a function of t for $t_w = 20$ min and $\Delta\rho = 1806\,\mathrm{kg/m^3}$ (solid squares) and $1151\,\mathrm{kg/m^3}$ (open squares). (b) D/R as a function of t for $\Delta\rho = 1345\,\mathrm{kg/m^3}$ and, from left to right, $t_w = 1$, 2, 5, 10, 20, 30, 40, and 45 min. The dotted line again has a logarithmic slope of 1.

The sphere's behavior depends on the net gravitational force $F \propto \Delta\rho = \rho_s - \rho_l$ acting on it. For sufficiently large $\Delta\rho$ (Regime 1), the sphere reaches a steady-state speed as gravity becomes balanced by drag. For small $\Delta\rho$ (Regime 3), the speed of the sphere decreases to zero while the sphere moves a distance of order R. In the intermediate regime (Regime 2), the initial velocity v_i persists up to a displacement much larger than R, after which the sphere again slows and stops. The same three regimes are observed as t_w is increased for fixed $\Delta\rho$, as shown in fig. 1(b) [11].

[1]In the inset to fig. 1(a), $t = 0$ corresponds to the start of the experiment when the sample age is t_w. Elsewhere we have removed data from the inertial regime by a small shift of the time origin, so, for example, $t = 0$ is 0.8 s after the sphere enters the material in fig. 1(a). We also measure the penetration depth D relative to its value at this shifted time origin. This shift does not affect our results.

Figure 1(b) shows that v_i decreases with increasing t_w for a fixed $\Delta\rho$. The instantaneous speed v also decreases with t in Regimes 2 and 3, as the material continues to age. A naive description of the material as having an apparent viscosity which increases with time as the structure in the suspension redevelops is inconsistent with the data, however: For both of the two largest t_w values plotted in fig. 1(b), the sphere starts to slow significantly after about 100 s, much shorter than the 5 min difference in t_w between these two trials. If the stoppage were due to an increase in viscosity, this viscosity would have to increase much more over the 100 s of motion than over the additional 5 min of aging. This contradiction shows that a closer look is required.

Our results in fact indicate that the state of the material and the flow around the moving sphere are very different in the three regimes. The overall deformation γ of the suspension in Regime 3 is of order $2R/L \approx 0.2$. As discussed below, this is close to the critical deformation γ_c at which our suspension undergoes the solid-to-liquid transition [16], suggesting that our suspension remains a solid in Regime 3. In Regime 1, in contrast, $\gamma \gg \gamma_c$ and the material around the sphere is quickly fluidized. It is also initially fluidized in Regime 2, but here the material structure redevelops on a time scale similar to that of the experiment, leading to a transition from liquid to solid over the course of the run. This description is consistent with, for example, the data for $t_w = 30$ (in Regime 2) and 40 min (in Regime 3). In the former case, the sphere stops after about 600 s because the material has changed from liquid to solid, while in the latter case the material is solid at the start of the run. The material becomes solid at about the same age —approximately 40 min— in both cases.

In Regimes 1 and 2, v_i depends on the state of development of the microstructure, and so on t_w. v_i is not zero in Regime 3, however, as seen in figs. 1(a) and (b), so there is a minimum speed $v_c \sim 1$ mm/s that can be reached in the liquid regime. If $v_i < v_c$, the material is in its solid regime, steady motion of the sphere is not possible, and it comes quickly to a stop[2].

The rheological properties of our suspension were measured with a controlled-strain rheometer, using a 50 mm parallel-plate tool (plate separation 1.5 mm) covered with sand-paper to prevent slip[3]. Following a preshear to rejuvenate the sample, we measured the stress τ as a function of $\dot\gamma$, starting from high $\dot\gamma$ and working downwards to limit the effects of aging on the measurements. We waited 15 s at each value of $\dot\gamma$. The resulting flow curve is shown by the crosses in fig. 2.

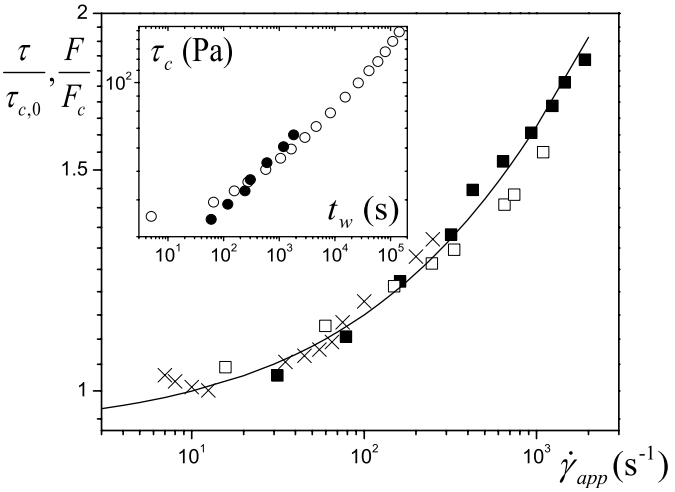

Fig. 2: Crosses: $\tau/\tau_c(0)$ as a function of $\dot\gamma_{app}$ for the Laponite suspension in simple shear. Squares: F/F_c *vs.* v/ℓ obtained from the falling-sphere experiments with $t_w = 4$ min (solid squares) and 20 min (open squares). The curve is a fit of eq. (4) to the force data. The inset shows the increase of the apparent yield stress τ_c with age determined from $G'(t_w)$ (open circles) and $F_c(t_w)$ (solid circles). The values of k_c and ℓ used in this analysis are discussed in the text.

We consistently observed a minimum in τ at $\dot\gamma_c \approx 20\,\mathrm{s}^{-1}$. This may indicate the presence of shear-banding at lower $\dot\gamma$, as has been observed in other thixotropic materials [17]. We neglect the data in this low-shear-rate region and take only that for $\dot\gamma > \dot\gamma_c$ as reflecting the behavior of the homogeneous material. We take the value of τ at the minimum as an estimate of the yield stress at $t_w = 0$. The apparent instability of uniform shear flow below γ_c may be analogous to our observation that steady motion of the falling sphere is not possible for $v < v_c$, suggesting that flow instabilities analogous to shear-banding are not restricted to simple viscometric flows.

The elastic modulus $G'(t_w)$ was measured under oscillatory shear at angular frequency $\omega = 1$ rad/s and strain amplitude 5%. G' was independent of ω for $0.1 < \omega < 100$ rad/s. For all waiting times, G' is constant at low-strain amplitudes, and its low-strain value $G'(0, t_w)$ increased significantly with t_w. G' decreases at higher strains as the material becomes fluidized. For all $t_w \leqslant 4800$ s, G' falls to 2/3 of $G'(0, t_w)$ at a strain of 0.2, which we take as the yield strain γ_c. This value of γ_c is consistent with results from creep tests on other pasty materials [16]. γ_c decreases slightly for $t_w > 4800$ s.

Taking the material to be viscoelastic in the solid regime, the yield stress is given by $\tau_c(t_w) = G'(0, t_w)\gamma_c$. We find $\tau_c(0) = 34$ Pa, consistent with the value estimated from the minimum in the flow curve. The stress data in fig. 2 have been normalized by this value, and $\tau_c(t_w)$ is plotted in the inset to fig. 2. The yield stress increases smoothly with t_w with a logarithmic slope that increases as the material ages.

[2]There can be no truly steady motion in a material in which the yield stress increases with age. Our meaning here is simply that the measured velocity remains constant over the duration of the experiment.

[3]While the shear stress in the parallel-plate geometry is inhomogeneous, it is shown in ref. [3] that the flow curve measured with parallel plates is very close to that measured with a thin-gap Couette geometry, in which the stress is more homogeneous. It is simpler to reduce the effects of wall slip in the parallel-plate geometry.

We can describe the net force F on our sphere by

$$F/F_c(t_w) = a + b\dot{\gamma}_{app}^n \tag{4}$$

for $F > F_c$. This is similar to eq. (2) [9], but here F_c depends on t_w and a and b are treated as parameters. A fit of eq. (4) to our falling-sphere data gives $a = 0.93$, less than the value of 1 expected for non-aging yield-stress fluids. Thus the shear rate, and so the speed v of the sphere, is greater than zero when $F = F_c$, consistent with the results discussed above. F/F_c is plotted against $\dot{\gamma}_{app}$ for two values of t_w in fig. 2. To make the force data consistent with the rheometric flow curve, we had to take $\ell = 0.009R$ in the calculation of $\dot{\gamma}_{app}$, a factor of 100 smaller than for non-aging yield-stress fluids. This suggests that the sheared region around the moving sphere is very thin for our aging material.

Using eq. (3) and the data in fig. 1(b), we can determine $F_c(t_w)$ for a given $\Delta\rho$. We then calculate the corresponding yield stress using eq. (3). We again find that τ_c increases with t_w, but to get agreement between the yield stress values determined from the falling-sphere data and those obtained from the measurements of G', we are forced to take $k_c = 1.085$ in eq. (3). This is much less than the value for non-aging yield-stress fluids, and close to what is calculated from eq. (1) if S_c coincides with the surface of the sphere [18]. This is further evidence that the moving sphere fluidizes only a thin layer of the suspension, with the smallness of k_c due to the fact that less force is required to disrupt the structure of a smaller volume of material. We emphasize that the low values of k_c and ℓ do not depend on any choice of constitutive relation, but are required to make the falling-sphere data consistent with the rheometric measurements.

These results indicate that the fluidized layer is very thin for our aging suspension, while in contrast it is known to extend approximately R from the surface of the sphere for non-aging yield-stress fluids [2,10]. One would expect this to result in significant irreversible flow ahead of the sphere in the latter case, but not in the former. We confirmed this by tracking the motion of 360 μm glass beads suspended in the material and illuminated by a laser sheet. Figure 3 shows the displacement of an initially horizontal line of tracer particles due to the slow passage of the sphere in both a Laponite suspension (solid squares) and a non-aging Carbopol gel [3] (crossed squares) (here $F/F_c = 1.5$). The displacement calculated for a Newtonian fluid [19] is also shown as a solid line. Both the vertical and horizontal displacements are much smaller in the Laponite suspension than in the Carbopol or the Newtonian fluid, and the displacements in the Laponite do not change significantly as the nominal shear rate v/R is varied from $1\,\mathrm{s}^{-1}$ to $30\,\mathrm{s}^{-1}$. The inset to fig. 3 shows the trajectory of a single particle initially located $R/3$ from a vertical line through the center of the sphere in the Laponite suspension. This particle moves horizontally to let the sphere pass by, then nearly returns to its initial position, but is not significantly displaced vertically. This indicates that the material in which the particle sits is primarily deformed elastically but does not undergo significant irreversible flow, confirming that the extent of the fluidized layer around the sphere is much less than in the other materials.

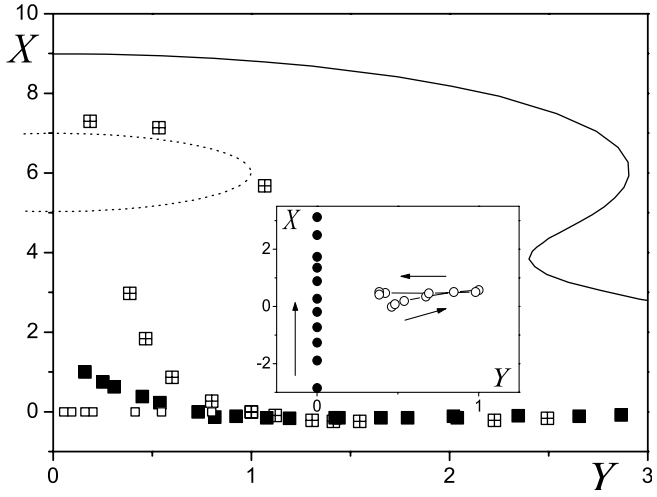

Fig. 3: Displacement X of a line of trace particles initially at $X = 0$ after the sphere moves from $X = -3$ to $X = 6$, plotted against the distance Y from the axis of the sphere. X and Y are in units of R. Solid squares: a Laponite suspension similar to that described in the text; G' is 1.5 times larger due to two months additional storage prior to use. Here $R = 1.26\,\mathrm{cm}$ and $v/R = 1.5\,\mathrm{s}^{-1}$. Crossed squares: Carbopol, a non-aging yield-stress fluid [3]; $R = 1.96\,\mathrm{cm}$ and $v/R = 0.57\,\mathrm{s}^{-1}$. The initial positions of seven of these particles, corresponding to the seven with the largest X displacement, are shown as open squares to emphasize that both lateral displacements and displacements in the direction of motion are significant in this case. Solid line: calculated displacements for a Newtonian fluid with no wall effects; here the results do not depend on v. The final position of the sphere is shown by the dotted line. The inset shows the position of a particular tracer particle in the Laponite suspension at successive times (open circles) and the corresponding locations of the sphere's center (solid circles).

We have shown that the fluidized region around a moving sphere is approximately two orders of magnitude thinner in a suspension which exhibits rheological aging than in non-aging pasty materials. This is a result of the aging itself and is directly related to the result shown in figs. 1 and 2 that there is no steady flow below a critical speed. Away from the moving sphere the shear rate is small, so the fluid structure reforms and the material becomes solid. Closer to the sphere, however, the higher shear rates keep the material fluidized [11]. While our findings remain to be confirmed in other similar materials and details such as the role of elasticity have yet to be explored, our results are expected to be relevant to understanding the motion of objects in yield-stress materials in general. We studied the motion of a

macroscopic sphere, but similar behavior may occur on much smaller scales around microscopic particles diffusing within the suspension [20], or even around the colloidal particles that make up the suspension itself, since the stresses involved are of the same order of magnitude.

* * *

We thank T. Toplak for his contributions. This research was supported by NSERC of Canada. PC acknowledges receipt of a visiting fellowship from the Center for Chemical Physics at UWO.

REFERENCES

[1] Coussot P., *Rheometry of pastes, suspensions and granular materials* (Wiley, New York) 2005.
[2] Beris A. N. *et al.*, *J. Fluid Mech.*, **158** (1985) 219.
[3] Tabuteau H., Coussot P. and de Bruyn J. R., *J. Rheol.*, **51** (2007) 127.
[4] Coussot P. *et al.*, *Phys. Rev. Lett.*, **88** (2002) 218301; Varnik F. *et al.*, *Phys. Rev. Lett.*, **90** (2003) 095702.
[5] Sollich P. *et al.*, *Phys. Rev. Lett.*, **78** (1997) 2020.
[6] Derec C. *et al.*, *C. R. Acad. Sci. Paris IV*, **1** (2000) 1115; Ramos L. and Cipelletti L., *Phys. Rev. Lett.*, **87** (2001) 245503; Cloitre M. *et al.*, *Phys. Rev. Lett.*, **90** (2003) 068303.
[7] Coussot P. *et al.*, *J. Rheol.*, **46** (2002) 573.
[8] Knaebal A. *et al.*, *Europhys. Lett.*, **52** (2000) 73; Bonn D. *et al.*, *Phys. Rev. Lett.*, **89** (2002) 015701; Bellour M. *et al.*, *Phys. Rev. E*, **67** (2003) 031405; Schosseler F. *et al.*, *Phys. Rev. E*, **73** (2006) 021401.
[9] Atapattu D. D., Chhabra R. P. and Uhlherr P. H. T., *J. Non-Newt. Fluid Mech.*, **59** (1995) 245.
[10] Beaulne M. and Mitsoulis E., *J. Non-Newt. Fluid Mech.*, **72** (1997) 55.
[11] Ferroir T. *et al.*, *Phys. Fluids*, **16** (2004) 594; Khaldoun A. *et al.*, *Nature*, **437** (2005) 635.
[12] Gueslin B., Talini L., Herzhaft B., Peysson Y. and Allain C., *Phys. Fluids*, **18** (2006) 103101.
[13] Southern Clay Products, Gonzalez, TX, `http://www.laponite.com`.
[14] Atapattu D. D., Chhabra R. P. and Uhlherr P. H. T., *J. Non-Newt. Fluid Mech.*, **38** (1990) 31.
[15] de Bruyn J. R., *Rheol. Acta*, **44** (2004) 150.
[16] Coussot P. *et al.*, *J. Rheol*, **50** (2006) 975.
[17] Pignon F., Magnin A. and Piau J. M., *J. Rheol.*, **40** (1996) 573; Coussot P. *et al.*, *Phys. Rev. Lett.*, **88** (2002) 175501; Bonn D. *et al.*, *Europhys. Lett.*, **59** (2002) 786.
[18] du Plessis M. P. and Ansley R. W., *J. Pipeline Div. ASCE*, **2** (1967) 1.
[19] Papanastasiou T., Georgiou G. and Alexandrou A., *Viscous Fluid Flow* (CRC Press, Boca Raton) 1999.
[20] Gardel M. L., Valentine M. T. and Weitz D. A., in *Microscale Diagnostic Analysis*, edited by Breuer K. (Springer Verlag, Berlin) 2005; Waigh T. A., *Rep. Prog. Phys.*, **68** (2005) 685.